

RESEARCH ARTICLE

Induction Patterns of an Extensin Gene in Tobacco upon Nematode Infection

Andreas Niebel,^a Janice de Almeida Engler,^a Christine Tiré,^a Gilbert Engler,^b Marc Van Montagu,^{a,1} and Godelieve Gheysen^a

^a Laboratorium voor Genetica, Universiteit Gent, K.L. Ledeganckstraat 35, B-9000 Gent, Belgium

^b Laboratoire Associé de l'Institut National de la Recherche Agronomique (France), Universiteit Gent, B-9000 Gent, Belgium

When sedentary endoparasitic nematodes infect plants, they induce complex feeding sites within the root tissues of their host. To characterize cell wall changes induced within these structures at a molecular level, we studied the expression of an extensin gene (coding for a major structural cell wall protein) in nematode-infected tobacco roots. Extensin gene expression was observed to be induced very early upon infection. This induction was weak, transient, and probably due to wounding during penetration and migration of the tobacco cyst nematode *Globodera tabacum* ssp *solanacearum*. In contrast, high extensin gene expression was observed during the whole second larval stage (an ~2-week-long phase of establishment of the feeding site) of the root knot nematode *Meloidogyne javanica*. During later stages of this interaction, expression gradually decreased. Extensin gene expression was found in at least three different tissues of the gall. We propose that distinct mechanisms lead to induced expression in these different cell types. The significance of these results for the understanding of plant–nematode interactions as well as the function of structural cell wall proteins, such as extensin, is discussed.

INTRODUCTION

One of the unique features of plant cells as opposed to animal cells is the presence of a rigid extracellular matrix, the cell wall. It plays an important structural role in plant architecture and in protection against mechanical and pathogenic stresses (for a review, see Varner and Lin, 1989; Carpita and Gibeau, 1993). The cell wall contains significant amounts of proteins (5 to 10% of the dry weight of primary cell walls) (Cassab and Varner, 1988). Among these, the extensins are one of the best-characterized and most abundant structural protein families. Extensins are basic proteins with a high content of glycosylated hydroxyproline residues. One of their typical features is the presence of repetitive amino acid sequences, among which serine(hydroxyproline)₄ is the most abundant one. Extensin genes have been characterized thoroughly in a large number of plants: carrot (Chen and Varner, 1985), bean (Corbin et al., 1987), oilseed rape (Evans et al., 1990), tomato (Showalter et al., 1991), and tobacco (Memelink, 1988). They are usually present as differentially regulated members of gene families (for a review, see Showalter and Rumeau, 1990).

Induction of extensin gene expression after a variety of stress situations, including wounding (Showalter et al., 1991), cold treatment (Weiser et al., 1990), and hypoxia (Rumeau et al., 1990), has been observed. The involvement of

hydroxyproline (Giebel and Stobiecka, 1974), and more specifically hydroxyproline-rich glycoproteins (HRGPs), in compatible and incompatible plant–pathogen interactions has received a great deal of attention (Esquerré-Tugayé et al., 1979; Showalter et al., 1985; Mazau and Esquerré-Tugayé, 1986). Whereas significant efforts have been devoted to studying HRGPs in plant–fungus (Benhamou et al., 1990a, 1991), plant–bacteria (O'Connell et al., 1990), and plant–virus (Benhamou et al., 1990b) interactions, to our knowledge, no work has been reported on HRGPs in plant–nematode interactions.

We focused on two species of nematodes that belong to families differing significantly in their parasitic behavior: the root knot nematodes (Meloidoderinae) and the cyst nematodes (Heteroderinae). To reach the xylem parenchyma in which they will establish their sophisticated feeding site, root knot nematodes first have to migrate toward the root tip where the absence of differentiated endodermis allows them to enter the vascular cylinder. This migration process, which happens intercellularly, causes only very limited necrotic lesions (Wyss et al., 1992). The nematodes finally start feeding on 3 to 10 cells of the vascular cylinder, which are rapidly turned into giant cells. These cells develop cell wall ingrowths, which are thought to increase solute uptake from the vascular system (Pate and Gunning, 1972; Jones, 1981). At the same time, the cells of the surrounding pericycle start to divide, giving rise to a typical

¹ To whom correspondence should be addressed.

swelling called root knot or gall. In contrast, cyst nematodes migrate intracellularly, directly toward the central cylinder, causing extensive necrosis. There, they start to feed upon a single cell that is rapidly turned into a large syncytium by incorporation of neighboring cells. Generally, no swelling is induced.

Rather than studying the involvement of HRGPs in the resistance mechanisms toward plant parasitic nematodes, we were interested in using extensin as a molecular marker to understand induced cell wall alterations observed during the different steps of a compatible plant–nematode interaction (penetration, migration, and especially induction and maintenance of a permanent feeding site after becoming sedentary). In this paper, we describe extensin gene expression in tobacco roots after infection by the root knot nematode *Meloidogyne javanica* and by the tobacco cyst nematode *Globodera tabacum* ssp *solanacearum*.

RESULTS

Extensin mRNA Levels Increase in Tobacco Roots upon Root Knot Nematode Infection

To compare extensin gene expression at different stages of the interaction between tobacco and root knot or cyst nematodes, we needed a synchronized infection system. For that purpose, we established an efficient *in vitro* inoculation system in tobacco for both parasites.

Total RNA was extracted from root knot nematode–induced galls 1, 2, and 3 weeks after inoculation, and the level of steady state extensin mRNA was assayed by RNA gel blot analysis. Extensin mRNA was already present at a higher level in tobacco roots as compared to the other organs of the plant (results not shown). Nevertheless, Figure 1 demonstrates that a clear-cut induction of extensin steady state mRNA was found upon root knot nematode infection. One week after infection (the nematodes were still in their second larval stage), the level of extensin mRNA had increased significantly as compared to that of uninfected roots (Figure 1). The mRNA level was still very high after 2 weeks (the nematodes were then at the end of their second or at the beginning of their third larval stage) and had decreased after 3 weeks of infection (the root knot nematodes were then at the adult stage). Three transcripts of 1.4, 3.5, and 6 kb were observed in both infected and control tissues (visible upon longer exposure; data not shown). However, none of these three transcripts was observed to be preferentially induced, and their expression pattern upon infection seemed coordinated. Multiple bands are a common feature for extensin RNA gel blots and probably reflect cross-hybridization between different extensin family members. Tobacco contains several extensin genes (Memelink, 1988), one of them being highly homologous to a *Nicotiana plumbaginifolia* gene that we have used as a probe (De Loose et al., 1991). The main band observed in Figure 1 (1.4 kb) presumably results from the induction of this gene.

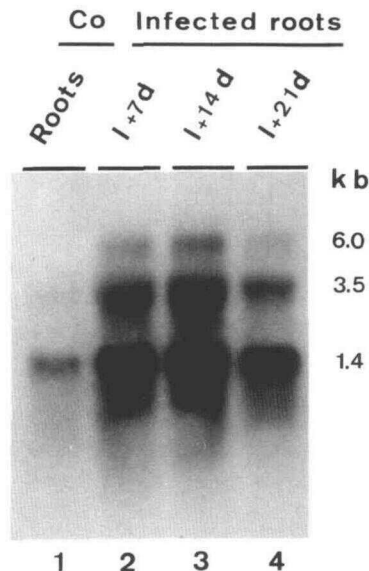


Figure 1. RNA Gel Blot Analysis of Extensin mRNA.

Lane 1 contains 5 μ g of total RNA from uninfected tobacco roots; lanes 2, 3, and 4 contain 5 μ g of total RNA from root knot nematode–infected roots 7, 14, and 21 days after inoculation, respectively. Co, control.

By means of RNA gel blot analysis, we showed that root knot nematode infection induces high levels of extensin gene expression in tobacco roots. Although this induction was very high after 1 and 2 weeks of the parasite cycle inside roots, the steady state mRNA level had already started to decrease 3 weeks after inoculation.

Extensin mRNA Is Strongly Induced in the Cortical Region of Root Knot Nematode–Induced Galls

To determine in which root tissues the extensin mRNA was localized upon nematode infection, *in situ* mRNA hybridizations were performed on tobacco galls collected 1, 2, and 3 weeks after inoculation with root knot nematodes. Figure 2 shows longitudinal sections of uninfected and infected root sectors hybridized with antisense extensin or control riboprobes. In all three stages of infection, extensin mRNA induction is clearly visible.

One week after infection, strong labeling could be found mainly in the gall cortex and in adjacent endodermal and pericycle layers, which start to divide upon infection (Figure 2). No strong extensin mRNA signal could be detected in the vascular parenchyma in which the root knot nematode became sedentary and induced giant cells. This pattern of expression was also seen 2 weeks after infection. Again, no strong extensin mRNA signal could be detected in the vascular parenchyma or in the giant cells induced by the nematode. In 3-week-old galls, a decrease in the intensity of labeling was observed in several sectors within the gall cortex region. This lower

expression in cells that contained high amounts of extensin mRNA in previous stages could account for the overall steady state mRNA decrease in infected tissue observed by RNA gel blot analysis at that stage (Figure 1). In all cases, labeling was restricted to the infection zone. Induction was never detected in uninfected sectors of infected roots.

By means of in situ mRNA hybridizations, we confirmed the temporal extensin gene expression pattern in root knot nematode-infected roots previously observed by RNA gel blot analysis. We also localized the majority of this induced extensin mRNA in root tissues in the vicinity but not in direct contact with the giant cells and, thus, the pathogen.

Induction of Extensin Transcription during Early Stages of the Tobacco-Root Knot Nematode Interaction

Because striking morphological changes induced in infected roots can already be observed during the early stages of infection, we decided to study extensin gene expression during the first days after inoculation. To do so, we performed root knot nematode infections on tobacco plants containing a chimeric construct consisting of the *N. plumbaginifolia* extensin promoter fused to the coding region of the β -glucuronidase (*gus*) gene (C. Tiré, R. De Rycke, M. De Loose, D. Inzé, M. Van Montagu, and G. Engler, unpublished data) and checked for induced *gus* expression. No induction could be detected 1 day after inoculation (data not shown). At this stage, the larvae were usually penetrating or migrating inside the roots toward the vascular cylinder. One day later, most of the larvae were inside the vascular cylinder. Figure 3 presents whole-mount histochemical GUS assay experiments. After a 4-hr incubation with 5-bromo-4-chloro-3-indolyl β -D-glucuronide, GUS staining was observed in the center of initiating galls (Figure 3B), whereas no staining was seen in control roots (Figure 3A). A clear correlation could be observed between *gus* expression and immobilization of the larvae and, consequently, between extensin gene induction and initiation of a feeding site. Four days after inoculation, galls had developed further (Figure 3C) and intense GUS staining could be seen.

The intensity of the GUS staining then continued to increase until ~1 week after infection when a plateau, lasting until at least 2 weeks after inoculation, was reached. It was already significantly lower after 3 weeks, and almost absent after 4 weeks and during later stages, confirming the temporal mRNA patterns observed so far with RNA gel blot analysis and mRNA in situ hybridization.

To localize the GUS staining more precisely, thin sections were made. In Figure 4, cross-sections through a 2-week-old gall (Figure 4B) and an uninfected tobacco root (Figure 4A) are shown. Similar expression patterns to those obtained by mRNA in situ hybridizations were observed. In Figure 4B, it appeared that most of the GUS staining was visible around an axis passing through the two xylem poles, which had been strongly pushed apart. Pericycle cells that divide along this

axis of greatest expansion of the gall contained the strongest GUS staining, together with adjacent and partially disorganized endodermis cells. Staining could also be detected, although at a weaker level, in the surrounding cortical cells and in giant cells (especially in parts of the giant cells in contact with the nematode). No significant GUS staining could be detected in the vascular parenchyma.

Localization of Extensin Protein in Root Knot Nematode-Infected Roots

To check whether the parasite also had an effect on extensin protein levels in infected tobacco roots, we performed immunolocalization experiments with a tobacco extensin monoclonal antibody (Meyer et al., 1988) using both light and electron microscopy.

Figure 5 shows the results of an immunolabeling experiment on cross-sections through a 2-week-old gall and a control root of the same age. There is clearly more silver precipitate present in the infected tissue (Figure 5B) than in the uninfected control roots (Figure 5A). Increased levels of extensin protein could be found in nearly all tissues of the gall. Labeling was particularly strong in the gall cortex and pericycle. Less label was present in the vascular parenchyma, even when localized expression could be seen around giant cells and nematodes. It is interesting to note that label was preferentially found in periclinal rather than anticlinal cell walls of the gall cortex, in other words, in cell walls facing the center of the gall (Figure 5B).

By using immunolabeling at the electron microscopic level, these observations could be confirmed and further documented. Labeling in uninfected roots was usually low. Figures 6, 7, and 8 present transmission electron micrographs of extensin immunolocalization in control roots and different parts of root knot nematode-induced galls. The only control tissue in which significant label could be found was the cortex, mainly at junctions between cortical cells (Figure 6D). This was probably due to the young age of these in vitro-grown roots. In galls, abundant labeling was found in most cortical cell walls (Figure 6B); slightly less but still significant label was present in the gall pericycle (Figure 6C). Hardly any label was observed in the vascular parenchyma (Figure 6A), except in zones of contact between the nematode and the plant. At such zones, label was present both in cell walls facing the parasite (Figure 7A) and in the space often observed between the plant cell wall and the cuticle of the nematode (Figure 7B). No significant label was found in the cell wall of giant cells and, in particular, not in the cell wall ingrowths (Figures 7C and 7D). Nevertheless, significant labeling could be observed in the cytosol of giant cells (Figure 7D), as well as in the vacuoles and cytosol of most cells exhibiting strong labeling in their cell wall (Figure 6B).

The analysis of the distribution of label in intercellular spaces yielded intriguing results. It was usually more abundant in cell walls than in the intercellular space of gall cells at a distance

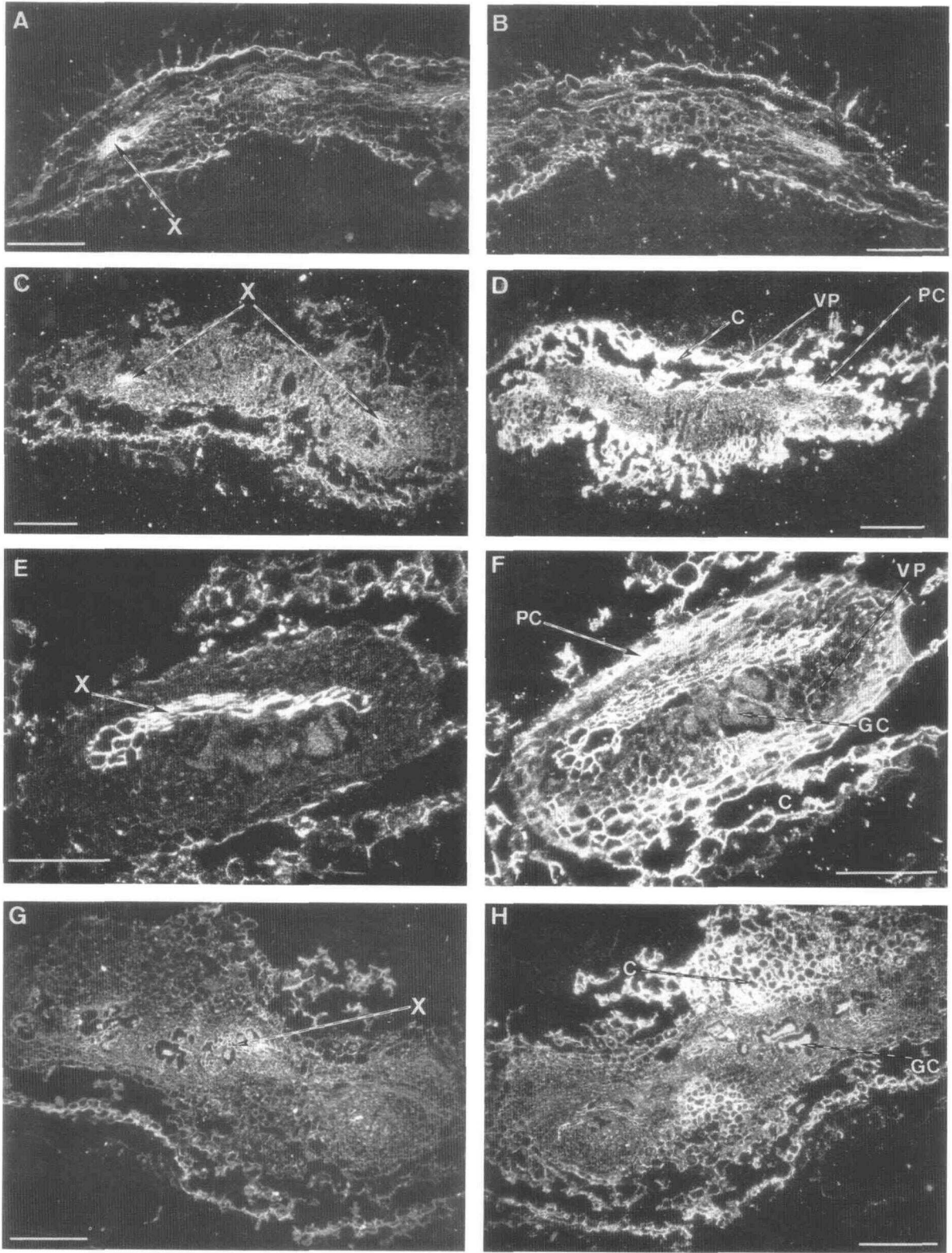


Figure 2. In Situ Hybridization of Extensin mRNA in Root Knot Nematode-Infected Tobacco Roots.



Figure 3. Whole-Mount Histochemical GUS Assays of Nematode-Infected and Uninfected Tobacco Roots.

Transgenic tobacco explants containing a chimeric construct consisting of the promoter of an *N. plumbaginifolia* extensin gene fused to the *gus* coding region were allowed to root in vitro, were infected with root knot or cyst nematodes, and were subsequently assayed for GUS activity.

(A) Uninfected tobacco root tip.

(B) Tobacco root tip 2 days after inoculation with root knot nematodes. The initiating gall can be seen just behind the root tip. Some larvae, which are still migrating through the root meristem at this stage, can be observed.

(C) Tobacco root sector 4 days after inoculation with root knot nematodes.

(D) Tobacco root sector a few hours after penetration of a tobacco cyst nematode larva.

(E) Necrotic tobacco root sector 1 week after tobacco cyst nematode inoculation.

L, larva; PS, penetration site. Bars = 125 μ m.

Figure 2. (continued).

(A) Longitudinal section through an uninfected root hybridized with a control riboprobe.

(B) Longitudinal section through an uninfected root hybridized with an antisense extensin riboprobe.

(C) Longitudinal section through a root infected with root knot nematodes hybridized with a control riboprobe, 1 week after inoculation.

(D) Longitudinal section through a root infected with root knot nematodes hybridized with an antisense extensin riboprobe, 1 week after inoculation.

(E) As shown in (C), 2 weeks after inoculation.

(F) As shown in (D), 2 weeks after inoculation.

(G) As shown in (C), 3 weeks after inoculation.

(H) As shown in (D), 3 weeks after inoculation.

The nematodes are not visible on these sections but are localized in the immediate vicinity of the giant cells. The bright appearance of the xylem is not a signal but an artifact of dark-field microscopy. C, cortex; GC, giant cell; PC, gall pericycle; VP, vascular parenchyma; X, xylem. Bars = 250 μ m.

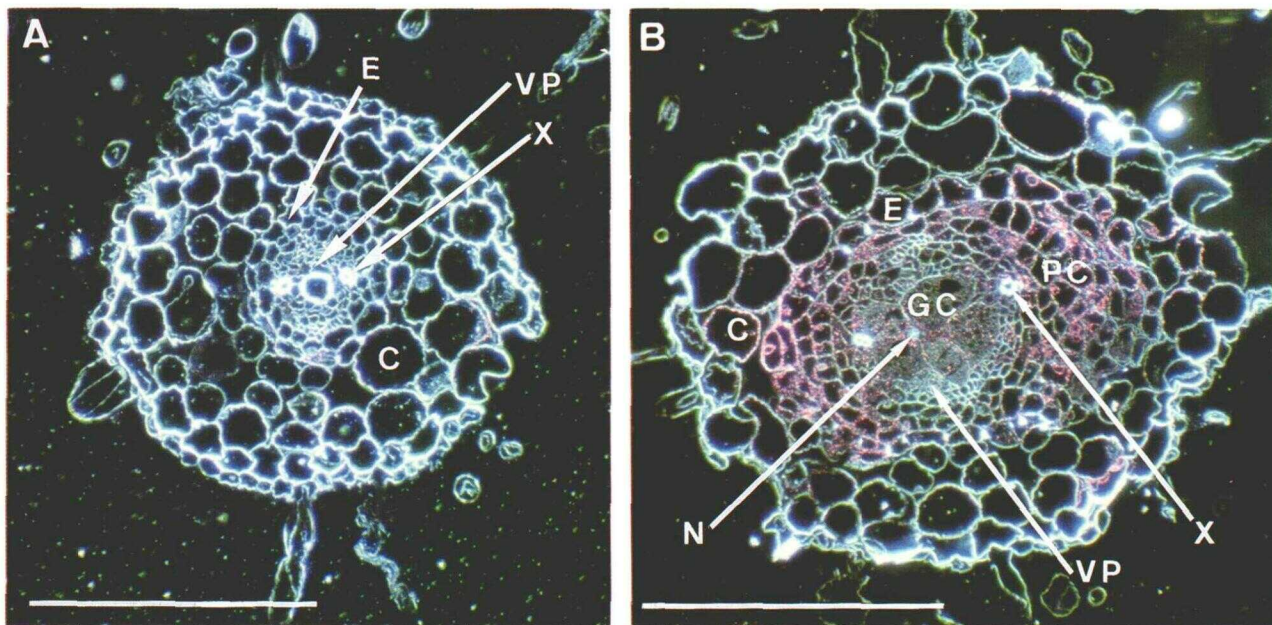


Figure 4. Histochemical GUS Assays of Nematode-Infected and Uninfected Tobacco Roots.

(A) Cross-section through an uninfected tobacco root.

(B) Cross-section through a tobacco gall 2 weeks after infection with root knot nematodes.

Only one of five giant cells is labeled. C, cortex; E, endodermis; GC, giant cell; N, nematode; PC, gall pericycle; VP, vascular parenchyma; X, xylem. Bars = 250 μm .

from the nematode, for instance in cortical cells (Figure 8A). Increasing amounts of gold particles were, however, detected in the intercellular spaces when moving closer to the pathogen. For example, in gall pericycle cells (Figure 8B), label could be found both in the cell wall and in the intercellular space. Finally, labeling was particularly intense in the intercellular space of the pericycle (Figure 8C) or of the vascular parenchyma (Figure 8D) cells very close to or in contact with nematodes (Figures 7A and 7B) or giant cells (Figures 8C and 8D).

Induction of Extensin in Tobacco upon Cyst Nematode Infection

When RNA gel blot analysis and in situ hybridizations were performed on tobacco roots infected for 1, 2, or 3 weeks by the tobacco cyst nematode, no significant increase in the extensin mRNA could be detected (data not shown). Figures 3D and 3E show the analysis of transgenic *gus* plants after cyst nematode infection. GUS staining could only be detected at penetration sites (Figure 3D) and along necrotic lesions due to the destructive intracellular migration of the nematode through the roots (Figure 3E). GUS staining could not be detected at any other point of the nematode cycle in the roots.

This extensin induction pattern could be further documented by protein immunolocalizations. Figure 5C shows the result

of an immunolabeling experiment on a cross-section through such a necrotic root sector 1 week after infection. The damage due to the destructive migration of several cyst nematode larvae is obvious here. The different tissues are disorganized, and some labeling can be found around the enlarged necrotic holes at the interface between cortex and vascular cylinder resulting from these migrations. Light micrographs showed that labeling was observed only in these necrotic tissues and not at feeding sites during later stages, which confirmed the data obtained with the histochemical GUS assay.

DISCUSSION

To understand more about the important cell wall modifications induced by plant parasitic nematodes in plant roots (Jones, 1981), we chose to study the expression of an extensin gene upon nematode infection.

RNA gel blot analysis, in situ hybridization, and histochemical GUS assays demonstrated a strong extensin gene expression upon infection with root knot nematodes. This was not observed upon infection by tobacco cyst nematodes. In the latter case, the restricted induction of GUS and extensin protein along necrotic penetration and migration lesions (Figures 3D, 3E, and 5C) is likely to be a response to wounding. This is not the case for root knot nematodes. First, damage

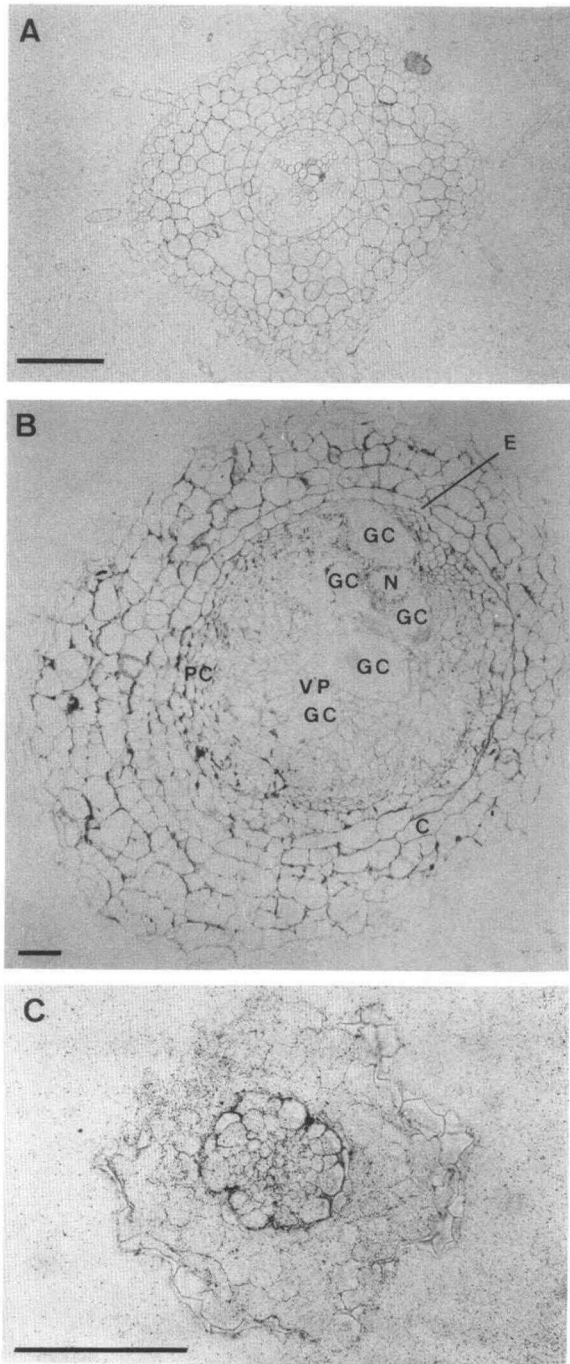


Figure 5. Light Micrographs of Protein Immunolabeling Using 11D2, a Tobacco Extensin Monoclonal Antibody.

- (A) Cross-section through an uninfected tobacco root.
 (B) Cross-section through a tobacco gall 2 weeks after root knot nematode infection.
 (C) Cross-section through a necrotic root sector 1 week after tobacco cyst nematode inoculation.
 C, cortex; E, endodermis; GC, giant cell; N, nematode; PC, gall pericycle; VP, vascular parenchyma. Bars = 125 μ m.

to host tissue during intercellular migrations is much lower. Hardly any root cells are killed by root knot nematode larvae, whereas most cells through which cyst nematodes move become necrotic. Second, GUS staining was never found along migration paths of root knot nematodes through roots. Early *gus* induction was always associated with larvae that had become sedentary. This indicates that cell wall changes specific to root knot nematode infection must occur during the first steps of feeding site initiation by this parasite. Extensin can thus be considered as a marker for initial root knot nematode-induced cell wall changes in infected roots.

An increase in extensin gene expression was also detected in later steps of the tobacco-root knot nematode interaction. When the parasite life cycle within the root was taken into account, a clear correlation could be found between the time of highest GUS staining intensity and larval stage 2. During this second larval stage, the nematode feeding site was initiated and, normally, fully established. Giant cells usually develop to full size before the second molt. Once these were totally functional and allowed the adult nematode to feed and reproduce, extensin gene expression started to decrease. Extensin can thus be considered as a molecular marker not only for initiation but also for the "building-up phase" of root knot nematode-induced feeding sites in roots.

Taking into account the mRNA, the GUS staining, and the protein localization data obtained by both light and electron microscopy, we can conclude that the extensin gene is induced in at least three different gall tissues. First, induction of extensin protein and GUS can be seen at a low yet significant level in the vascular parenchyma, but only in cells that are in direct contact with the pathogen or the giant cells (Figures 4B, 7A, 7B, and 8D). This induction is particularly obvious because significant amounts of extensin protein, GUS, and mRNA were never detected in vascular parenchyma cells of both control roots and parts of galls that were not in direct contact with the parasite (Figures 2, 4B, 5B, and 6A). The second type of tissue in which high induction levels could be found and that was only occasionally in direct contact with nematodes or giant cells was the gall pericycle. Finally, high protein levels and significant extensin steady state mRNA accumulation could be detected in the gall cortex some distance from the nematode. We believe that at least three different mechanisms lead to extensin gene induction in these three gall tissues.

First, for the expression in tissues in contact with the parasite, we are probably dealing with a direct response of the plant to the presence of the nematode. Localized induction of extensin proteins has been documented in several compatible and incompatible plant-fungi (Benhamou et al., 1991) or plant-bacteria (Mazau and Esquerré-Tugayé, 1986; O'Connell et al., 1990) interactions, both in regions of contact with the pathogen and in the neighboring intercellular space. We thus expected to observe a similar phenomenon upon nematode infection. Secretion of pathogenesis-induced proteins in general and extensin in particular to intercellular spaces is thought to be a way of controlling the invasion of this easily accessible compartment by different pathogens. Extensin has

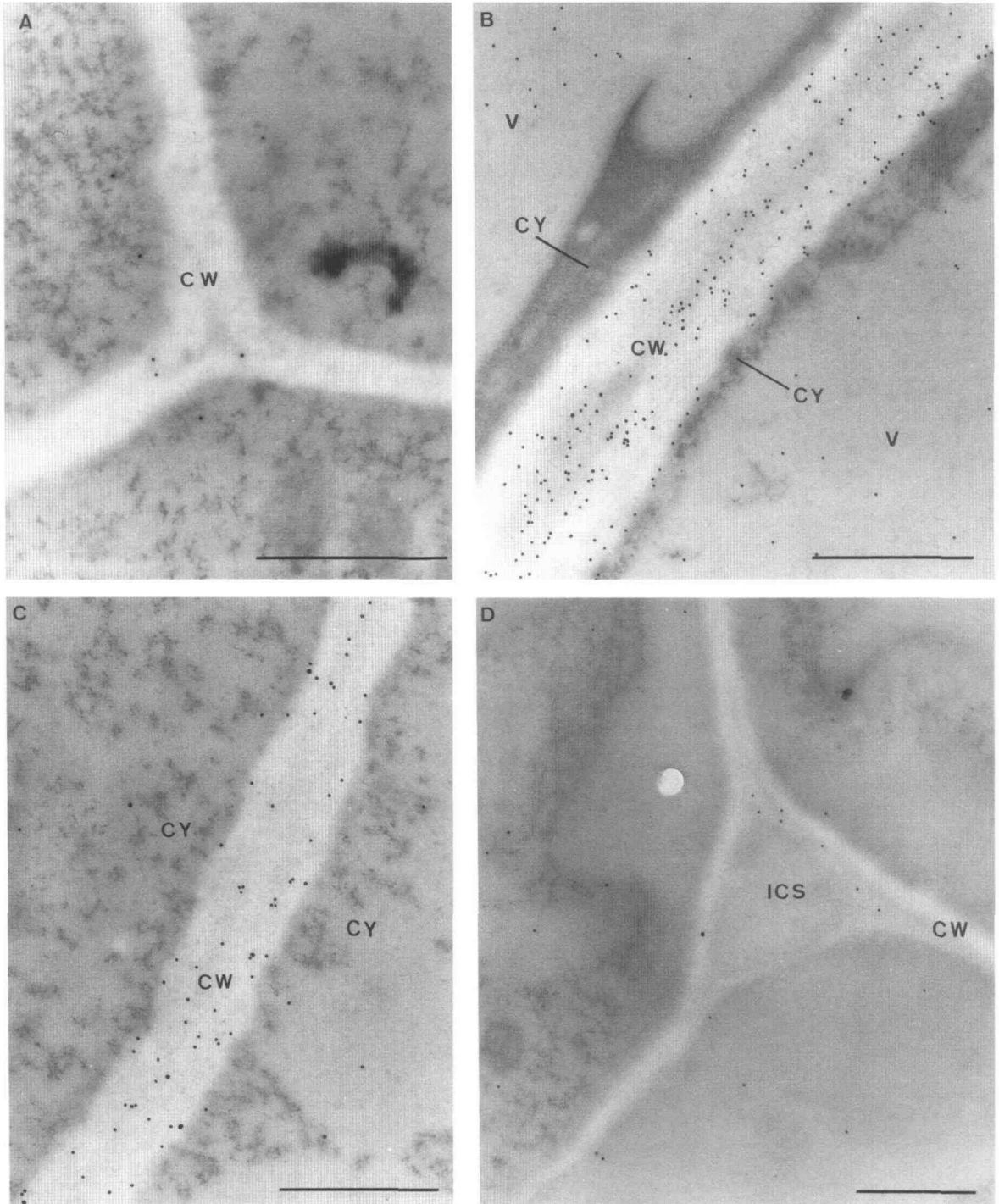


Figure 6. Transmission Electron Micrographs of Extensin Immunolocalization.

(A) Cell walls of gall vascular parenchyma 2 weeks after root knot nematode infection.

(B) Cell walls of gall cortical cells 2 weeks after infection with root knot nematodes.

(C) Cell walls of gall pericycle cells 2 weeks after infection with root knot nematodes.

(D) Cell walls of uninfected cortical root cells.

CW, cell wall; CY, cytoplasm; ICS, intercellular space; V, vacuole. Bars = 1 μm.

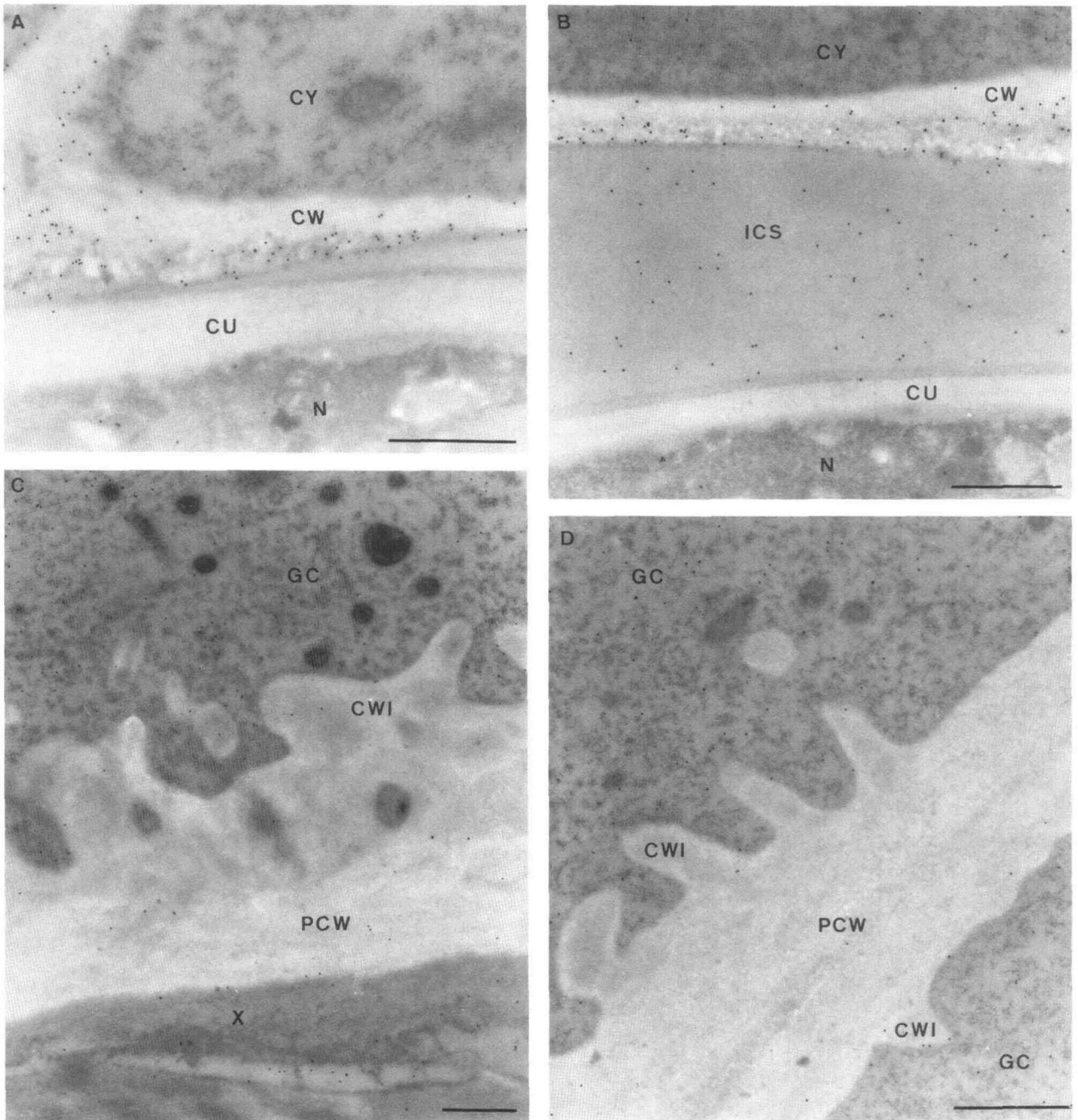


Figure 7. Transmission Electron Micrographs of Extensin Immunolocalization.

(A) Vascular parenchyma cells in contact with a root knot nematode.

(B) Intercellular space between a root knot nematode and a vascular parenchyma cell.

(C) Cell wall ingrowths at the interface between xylem and root knot nematode-induced giant cells.

(D) Cell wall ingrowths at the interface between two root knot nematode-induced giant cells.

CU, cuticle; CW, cell wall; CWI, cell wall ingrowth; CY, cytoplasm; GC, giant cell; ICS, intercellular space; N, nematode; PCW, primary cell wall; X, xylem. Bars = 1 μ m.

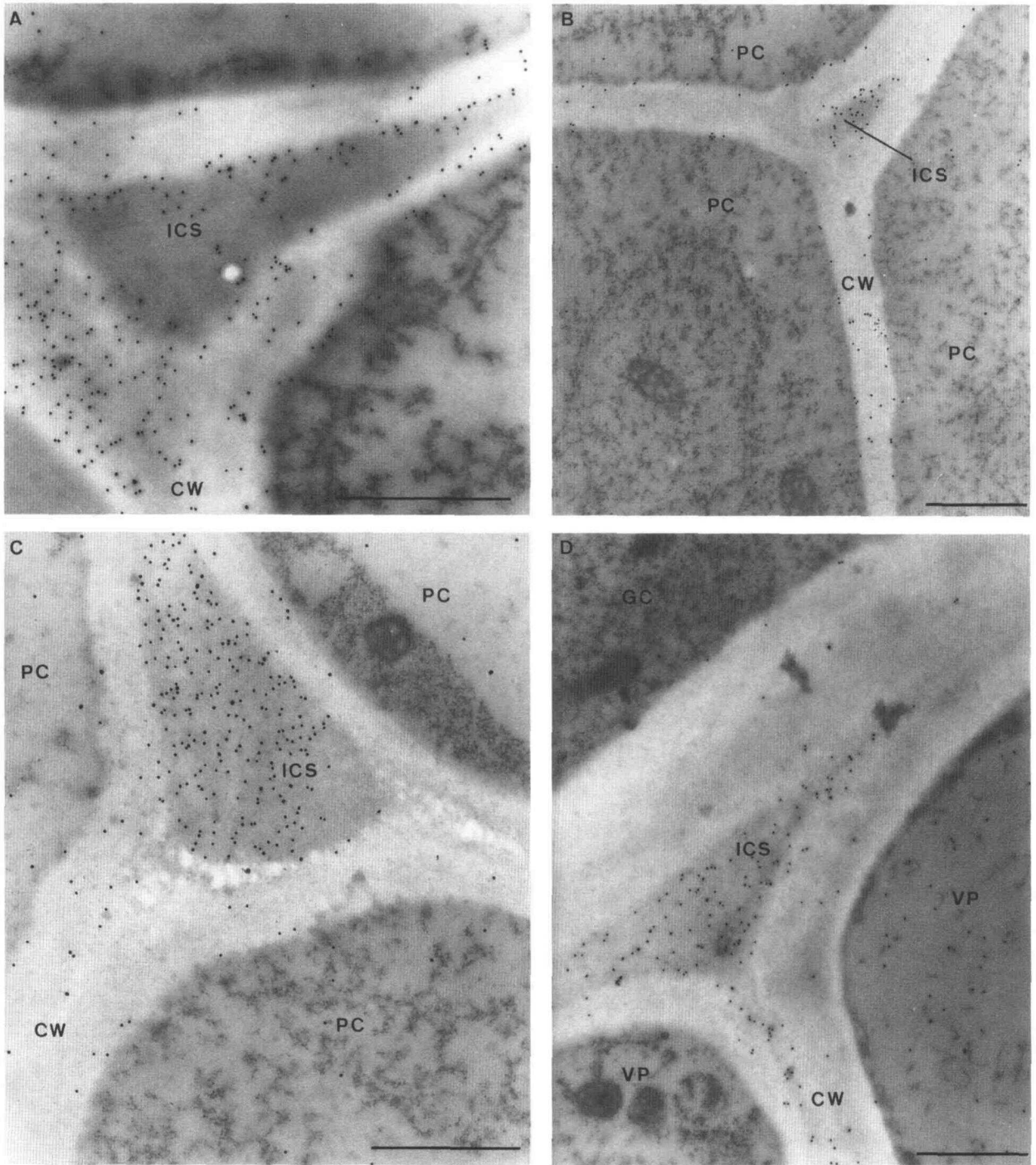


Figure 8. Transmission Electron Micrographs of Extensin Immunolocalization in the Intercellular Space.

(A) Intercellular space of gall cortex cells.

(B) Intercellular space of gall pericycle cells at a distance from the pathogen.

(C) Intercellular space of gall pericycle cells in the vicinity of a root knot nematode.

(D) Intercellular space of vascular parenchyma in contact with giant cells.

CW, cell wall; GC, giant cell; ICS, intercellular space; PC, gall pericycle cell; VP, gall vascular parenchyma cell. Bars = 1 μ m.

in this respect been proposed to play a potential role in building physical barriers by being cross-linked to itself and to other cell wall components. A role in agglutination of phytopathogenic bacteria has also been suggested (Mellon and Helgeson, 1982). In our case, especially when considering the gradient of extensin protein observed in the gall intercellular space (Figure 8), the induced levels of extensin could be interpreted as a response of the plant to the presence of "nonself" elements (i.e., the pathogenic root knot nematode) within its tissues. It is interesting to note that cells in contact with giant cells also exhibit this reaction. This might suggest that the plant would no longer consider these "redifferentiated" plant structures as being fully part of its own root tissue.

Second, in the gall pericycle, even when extensin induction is partially due to the presence of the nematode, there is probably an additional reason for the observed induction. Large amounts of extensin protein can be localized in intercellular spaces of this tissue but only when it is in the vicinity of a nematode or a giant cell (Figures 8B and 8C). Significant amounts of protein were found all over the cell walls of the gall pericycle, independent of the proximity of the pathogen. The additional cell layers of the gall pericycle are absent in uninfected roots. They are newly synthesized during the first 2 weeks after nematode infection through divisions of the original pericycle layer. High extensin gene expression has been detected in actively dividing cells in tobacco callus (A. Niebel and C. Tiré, unpublished data), tobacco crown galls (Memelink, 1988), and soybean root tips (Ye and Varner, 1991). Because extensin seems to play a role in neogenesis of cell walls, we propose that extensin gene expression in the gall pericycle is not only due to contact with the nematode but also that it is a consequence of the need for new structural cell wall components in dividing cells.

Finally, the induction of extensin in the cortical cells could have a third distinct origin. The gall cortex does not undergo cell divisions (A. Niebel, unpublished results), and no contact with the pathogen occurs after it has become sedentary. However, due to the presence of dividing pericycle cells, expanding giant cells, and growing nematodes, the central cylinder increases dramatically in volume, creating considerable mechanical pressure. Extensin has often been proposed to play a role in cell wall rigidity either by intermolecular cross-linking or by cross-linking with other cell wall components (Carpita and Gibeaut, 1993; Showalter, 1993). In this context, extensin gene expression has often been proposed to be induced as a result of mechanical stress. In *N. plumbaginifolia*, for example, the cortical cells around the leaf trace show high extensin gene expression (C. Tiré, R. De Rycke, M. De Loose, D. Inzé, M. Van Montagu, and G. Engler, unpublished data). Similarly, the hydroxyproline-rich glycoprotein HRGPnt3 of tobacco is strongly expressed in emerging lateral roots (Keller and Lamb, 1989). In our case, the cells of the gall cortex probably increased the rigidity of their walls (in particular by increasing their extensin contents) as a reaction to the mechanical pressure created by the swelling of the central cylinder.

In this way, the plant probably tries both to limit gall expansion and to maintain the coherence of its infected root tissue (galls sometimes burst open in case of massive infection). This hypothesis is strengthened by the preferential periclinal localization (thus facing the source of mechanical stress) of the extensin protein in the gall cortex cells (Figure 5B).

In the large cell walls of giant cells, significant amounts of protein could not be detected (Figures 7C, 7D, and 8D). This could illustrate the need for extensible cell walls in these expanding structures. In cell wall ingrowths (Figures 8C and 8D), which increase the surface of exchange between giant and defined neighboring cells, high solute uptake might be facilitated by a more loose organization of the cell wall resulting from the absence of a dense protein network.

Detailed study showed that the GUS staining localization in galls (2 weeks after inoculation) differed slightly from the extensin mRNA localization in situ hybridizations and from extensin protein immunolocalization. Indeed, the strongest GUS staining was observed in the gall pericycle. GUS staining was a little weaker in the gall cortex, although in this tissue high amounts of extensin mRNA and protein were localized. This could reflect the fact that with the transgenic *gus* plants we only observed the expression pattern of one particular extensin gene, whereas by using antibodies or mRNA probes we might have been localizing the products of several tobacco extensin genes.

Studying extensin expression upon root and cyst nematode infection in tobacco has allowed us to further understand the complex changes induced by these pathogens in roots and root cell walls. Galls that are formed after infection by root knot nematodes contain, within the same organ, most of the conditions that have been reported previously to lead to enhanced extensin expression: pathogen infection, cell wall neogenesis, and mechanical stress. Our findings further illustrate and thus confirm previous hypotheses about the possible functions of extensins in plants. Further work could be done to ascertain whether distinct extensin genes are induced in different gall tissues. Studying HRGPs with very precise developmental expression patterns would be of interest. Alternatively, the involvement of other cell wall proteins could be examined. In conclusion, we think that this system is interesting not only for plant pathologists but also for scientists trying to unravel the function of different cell wall components.

METHODS

Plant Material Preparation

One-internode stem cuttings of in vitro-grown tobacco (*Nicotiana tabacum* cv SR1) plants were allowed to root in Murashige and Skoog medium (Murashige and Skoog, 1962) containing 1% sucrose and 0.8% agar in Petri dishes. The roots grew toward the bottom of the dish where they spread, allowing easy nematode infection and subsequent observations.

Nematode Infections

Agrobacterium rhizogenes-transformed tomato (*Lycopersicon esculentum* cv Marmande) roots grown on B5 medium supplemented with 2% sucrose, pH 6.2, and 1.5% agar at 28°C (in the dark) were used to rear the root knot nematode *Meloidogyne javanica* axenically. Egg masses were collected, and the eggs were allowed to hatch in sterile water at room temperature. After 4 to 6 days, L2 stage larvae (the infective stage) were used for inoculation. For the cyst nematode *Globodera tabacum* ssp *solanacearum*, cysts were put into a 4-mM ZnCl₂ solution at room temperature to stimulate hatching. After 10 days, L2 stage larvae were collected and sterilized with a 0.1% HgCl₂ solution for 4 min and subsequently washed extensively with sterile water.

Inoculations were performed in the same way for both cyst and root knot nematodes. A 100- μ L suspension containing ~200 larvae was brought in direct contact with the roots by lifting the agar and applying the inoculum at the bottom of the Petri dish.

RNA Extraction and Gel Blot Analysis

Total RNA was extracted from freshly harvested in vitro-grown tobacco roots and galls, essentially as described by Jones et al. (1985). For RNA gel blot analysis, 5 μ g of total RNA was denatured in 10% formaldehyde, electrophoresed, and transferred to nylon membranes according to Maniatis et al. (1982). To verify that equal amounts of RNA were loaded in each lane, the concentration of all RNA solutions was first checked spectrophotometrically, and ethidium bromide was then added to each sample allowing a second verification on the gel prior to transfer. To obtain highly specific probes, a 1.8-kb fragment of the genomic clone of an *N. plumbaginifolia* extensin gene containing the entire coding sequence was subcloned into pGem2 and called Pext8 (C. Tiré, R. De Rycke, M. De Loose, D. Inzé, M. Van Montagu, and G. Engler, unpublished data), and ³²P-labeled single-stranded riboprobes were synthesized using the SP6 RNA polymerase.

RNA gel blot hybridizations were performed overnight at 68°C in 50% formamide, 3 \times SSC (1 \times SSC is 0.15 M NaCl, 0.015 M sodium citrate), pH 7.0, 0.25% nonfat milk powder, 0.5% SDS, 10% dextran sulfate, and 20 μ g/mL denatured herring sperm DNA. The filters were washed at 68°C for 20 min each, twice with 3 \times SSC, 0.5% SDS, once with 1 \times SSC, 0.5% SDS, once with 0.1 \times SSC, 0.5% SDS, and autoradiographed on Kodak XAR-5 films with intensifying screens for 1 to 10 hr at -70°C.

mRNA In Situ Hybridizations

³⁵S-labeled riboprobes were prepared from plasmid Pext8 (C. Tiré, R. De Rycke, M. De Loose, D. Inzé, M. Van Montagu, and G. Engler, unpublished data). Full-length transcripts were reduced to an average length of 0.1 to 0.15 kb by alkaline hydrolysis (Cox et al., 1984; Martineau and Taylor, 1986). The size of both full-length and hydrolyzed transcripts was checked on a 1% denaturing agarose gel, and the amount of synthesized RNA was calculated.

Infected and noninfected root pieces were fixed using a 0.1 M cacodylate buffer containing 0.3% glutaraldehyde and 4% paraformaldehyde, pH 7.4, for 3 hr. The tissue was then embedded in paraplast (Chadwick and McGinnis, 1987). Ten-micron sections were made with an Ultracut (Microtome 2000; Reichert-Jung GmbH, Nußloch, Germany) and pretreated according to the method of Cox et al. (1984). Hybridization of the probes to the slides was performed essentially as

described by Barker et al. (1988). Control sections were hybridized with a sense 2S albumin probe prepared from plasmid pEK1 (Krebbers et al., 1988). Autoradiography and developing were performed as described by Angerer and Angerer (1981).

Immunolabeling

For immunolabeling, roots were fixed with 4% paraformaldehyde and 0.3% glutaraldehyde for 3 hr at room temperature and incubated overnight at 4°C. After washing in a 0.2 M cacodylate buffer, pH 7.2, the tissue was gradually dehydrated with ethanol and embedded in LR white resin (London Resin, Basingstoke, U.K.). Samples were polymerized at -20°C with UV light. Thin and ultrathin sections were made using a diatome diamond knife. A monoclonal antibody, 11D2 (Meyer et al., 1988), kindly provided by David W. Galbraith (University of Arizona, Tucson, AZ) was used at a dilution of 1:2000 for all labeling experiments, which were done according to the method of De Clercq et al. (1990). Additionally, the Intense™ M Silver Enhancement Kit (Amersham, Aylesbury, U.K.) was used for light microscopy experiments. Micrographs were made using a Leitz Diaplan microscope (Wild, Heerbrugg, Switzerland) and Siemens 101 transmission electron microscope (Siemens AG, Karlsruhe, Germany). As a control in all immunolabeling experiments, another primary antibody, directed against phosphinothricin acetyl transferase, was used (De Block et al., 1987). Sections reacting with this polyclonal antibody showed virtually no signal.

Histochemical β -Glucuronidase Assays

Infected and noninfected root tissues were cut out from the Petri dishes at various time points after inoculation, and histochemical β -glucuronidase (GUS) assays were performed essentially according to the method of Jefferson et al. (1987). After a 4-hr incubation with 5-bromo-4-chloro-3-indolyl β -D-glucuronide at 37°C, the reaction was stopped, and whole-mount samples were photographed. In some cases, this material was fixed in 2.5% glutaraldehyde overnight at 4°C, subsequently embedded into LR white resin, and further processed according to the method of Peleman et al. (1989).

ACKNOWLEDGMENTS

We wish to thank Drs. David J. Meyer and David W. Galbraith for kindly providing the 11D2 tobacco monoclonal antibody, Prof. Charles S. Johnson for kindly providing cysts of *Globodera tabacum* ssp *solanacearum*, Tom Gerats, Dirk Inzé, and Fernanda de Carvalho for critical reading of the manuscript, Martine De Cock for help in preparing it, and Vera Vermaercke and Karel Spruyt for artwork. This work was supported by a grant from the "Vlaams Actieprogramma Biotechnologie" (No. 073). A. N. and J. d. A. E. are indebted to the Commission of the European Communities and the Conselho Nacional de Pesquisa for predoctoral and postdoctoral fellowships, respectively. G. E. is a Research Engineer of the Institut National de la Recherche Agronomique (France).

Received July 19, 1993; accepted September 30, 1993.

REFERENCES

- Angerer, L.M., and Angerer, R.C. (1981). Detection of polyA⁺ RNA in sea urchin eggs and embryos by quantitative in situ hybridization. *Nucl. Acids Res.* **9**, 2819–2840.
- Barker, S.J., Harada, J.J., and Goldberg, R.B. (1988). Cellular localization of soybean storage protein mRNA in transformed tobacco seeds. *Proc. Natl. Acad. Sci. USA* **85**, 458–462.
- Benhamou, N., Mazau, D., and Esquerré-Tugayé, M.-T. (1990a). Immunocytochemical localization of hydroxyproline-rich glycoproteins in tomato root cells infected by *Fusarium oxysporium* f. sp. *radicis-lycopersici*: Study of a compatible interaction. *Phytopathology* **80**, 163–173.
- Benhamou, N., Mazau, D., Esquerré-Tugayé, M.-T., and Asselin, A. (1990b). Immunogold localization of hydroxyproline-rich glycoproteins in necrotic tissue of *Nicotiana tabacum* L. cv. Xanthi-nc infected by tobacco mosaic virus. *Physiol. Mol. Plant Pathol.* **36**, 129–145.
- Benhamou, N., Mazau, D., Grenier, J., and Esquerré-Tugayé, M.-T. (1991). Time-course study of the accumulation of hydroxyproline-rich glycoproteins in root cells of susceptible and resistant tomato plants infected by *Fusarium oxysporum* f. sp. *radicis-lycopersici*. *Planta* **184**, 196–208.
- Carpita, N.C., and Gibeaut, D.M. (1993). Structural models of primary cell walls in flowering plants: Consistency of molecular structure with the physical properties of the walls during growth. *Plant J.* **3**, 1–30.
- Cassab, G.I., and Varner, J.E. (1988). Cell wall proteins. *Annu. Rev. Plant Physiol. Plant Mol. Biol.* **39**, 321–353.
- Chadwick, R., and McGinnis, W. (1987). Temporal and spatial distribution of transcripts from the *Deformed* gene of *Drosophila*. *EMBO J.* **6**, 779–789.
- Chen, J., and Varner, J.E. (1985). An extracellular matrix protein in plants: Characterization of a genomic clone for carrot extensin. *EMBO J.* **4**, 2145–2151.
- Corbin, D.R., Sauer, N., and Lamb, C.J. (1987). Differential regulation of a hydroxyproline-rich glycoprotein gene family in wounded and infected plants. *Mol. Cell. Biol.* **7**, 4337–4344.
- Cox, K., DeLeon, D.V., Angerer, L.M., and Angerer, R.C. (1984). Detection of mRNAs in sea urchin embryos by *in situ* hybridization using asymmetric RNA probes. *Dev. Biol.* **101**, 485–502.
- De Block, M., Botterman, J., Vandewiele, M., Dockx, J., Thoen, C., Gosselé, V., Movva, R., Thompson, C., Van Montagu, M., and Leemans, J. (1987). Engineering herbicide resistance in plants by expression of a detoxifying enzyme. *EMBO J.* **6**, 2513–2518.
- De Clercq, A., Vandewiele, M., De Rycke, R., Van Damme, J., Van Montagu, M., Krebbers, E., and Vandekerckhove, J. (1990). Expression and processing of an *Arabidopsis* 2S albumin in transgenic tobacco. *Plant Physiol.* **92**, 899–907.
- De Loose, M., Gheysen, G., Tiré, C., Gielen, J., Villarroel, R., Genetello, C., Van Montagu, M., Depicker, A., and Inzé, D. (1991). The extensin signal peptide allows secretion of a heterologous protein from protoplasts. *Gene* **99**, 95–100.
- Esquerré-Tugayé, M.-T., Lafitte, C., Mazan, D., Toppan, A., and Touzé, A. (1979). Cell surfaces in plant microorganism interactions. II. Evidence for the accumulation of hydroxyproline-rich glycoproteins in the cell wall of diseased plants as a defense mechanism. *Plant Physiol.* **64**, 320–326.
- Evans, I.M., Gatehouse, L.N., Gatehouse, J.A., Yarwood, J.N., Boulter, D., and Croy, R.R.D. (1990). The extensin gene family in oilseed rape (*Brassica napus* L.): Characterisation of sequences of representative members of the family. *Mol. Gen. Genet.* **223**, 273–287.
- Giebel, J., and Stobiecka, M. (1974). Role of amino acids in plant tissue response to *Heterodera rostochiensis*. I. Proline-proline and hydroxyproline content in roots of susceptible and resistant solanaceous plants. *Nematologica* **20**, 407–414.
- Jefferson, R.A., Kavanagh, T.A., and Bevan, M.W. (1987). GUS fusions: β -Glucuronidase as a sensitive and versatile gene fusion marker in higher plants. *EMBO J.* **6**, 3901–3907.
- Jones, J.D.G., Dunsmuir, P., and Bedbrook, J. (1985). High level expression of introduced chimaeric genes in regenerated transformed plants. *EMBO J.* **4**, 2411–2418.
- Jones, M.G.K. (1981). The development and function of plant cells modified by endoparasitic nematodes. In *Plant Parasitic Nematodes*, Vol. III, B.M. Zuckerman and R.A. Rohde, eds (New York: Academic Press), pp. 255–279.
- Keller, B., and Lamb, C.J. (1989). Specific expression of a novel cell wall hydroxyproline-rich glycoprotein gene in lateral root initiation. *Genes Dev.* **3**, 1639–1646.
- Krebbers, E., Herdies, L., De Clercq, A., Seurinck, J., Leemans, J., Van Damme, J., Segura, M., Gheysen, G., Van Montagu, M., and Vandekerckhove, J. (1988). Determination of the processing sites of an *Arabidopsis* 2S albumin and characterization of the complete gene family. *Plant Physiol.* **87**, 859–866.
- Maniatis, T., Fritsch, E.F., and Sambrook, J. (1982). *Molecular Cloning: A Laboratory Manual*. (Cold Spring Harbor, NY: Cold Spring Harbor Laboratory Press).
- Martineau, B., and Taylor, W.C. (1986). Cell-specific photosynthetic gene expression in maize determined using cell separation techniques and hybridization *in situ*. *Plant Physiol.* **82**, 613–618.
- Mazau, D., and Esquerré-Tugayé, M.-T. (1986). Hydroxyproline-rich glycoprotein accumulation in the cell walls of plants infected by various pathogens. *Physiol. Mol. Plant Pathol.* **29**, 147–157.
- Mellon, J.E., and Helgeson, J.P. (1982). Interaction of a hydroxyproline-rich glycoprotein from tobacco callus with potential pathogens. *Plant Physiol.* **70**, 401–405.
- Memelink, J. (1988). *Altered Gene Expression in T-DNA Transformed Tobacco Tissues*. Ph.D. Dissertation (Leiden, The Netherlands: Universiteit Leiden).
- Meyer, D.J., Afonso, C.L., and Galbraith, D.W. (1988). Isolation and characterization of monoclonal antibodies directed against plant plasma membrane and cell wall epitopes: Identification of a monoclonal antibody that recognizes extensin and analysis of the process of epitope biosynthesis in plant tissues and cell cultures. *J. Cell Biol.* **107**, 163–175.
- Murashige, T., and Skoog, F. (1962). A revised medium for rapid growth and bioassays with tobacco tissue cultures. *Physiol. Plant.* **15**, 473–497.
- O'Connell, R.J., Brown, I.R., Mansfield, J.W., Bailey, J.A., Mazau, D., Rumeau, D., and Esquerré-Tugayé, M.-T. (1990). Immunocytochemical localization of hydroxyproline-rich glycoproteins accumulating in melon and bean at sites of resistance to bacteria and fungi. *Mol. Plant-Microbe Interact.* **3**, 33–40.
- Pate, J.S., and Gunning, B.E.S. (1972). Transfer cells. *Annu. Rev. Plant Physiol.* **23**, 173–196.

- Peleman, J., Boerjan, W., Engler, G., Seurinck, J., Botterman, J., Allotte, T., Van Montagu, M., and Inzé, D.** (1989). Strong cellular preference in the expression of a housekeeping gene of *Arabidopsis thaliana* encoding S-adenosylmethionine synthetase. *Plant Cell* **1**, 81–93.
- Rumeau, D., Maher, E.A., Kelman, A., and Showalter, A.M.** (1990). Extensin and phenylalanine ammonia-lyase gene expression altered in potato tubers in response to wounding, hypoxia, and *Erwinia carotovora* infection. *Plant Physiol.* **93**, 1134–1139.
- Showalter, A.M.** (1993). Structure and function of plant cell wall proteins. *Plant Cell* **5**, 9–23.
- Showalter, A.M., and Rumeau, D.** (1990). Molecular biology of the plant cell wall hydroxyproline-rich glycoproteins. In *Organization and Assembly of Plant and Animal Extracellular Matrix*, W.S. Adair and R.P. Mecham, eds (New York: Academic Press), pp. 247–281.
- Showalter, A.M., Bell, J.N., Cramer, C.L., Bailey, J.A., Varner, J.E., and Lamb, C.J.** (1985). Accumulation of hydroxyproline-rich glycoprotein mRNAs in response to fungal elicitor and infection. *Proc. Natl. Acad. Sci. USA* **82**, 6551–6555.
- Showalter, A.M., Zhou, J., Rumeau, D., Worst, S.G., and Varner, J.E.** (1991). Tomato extensin and extensin-like cDNAs: Structure and expression in response to wounding. *Plant Mol. Biol.* **16**, 547–565.
- Varner, J.E., and Lin, L.-S.** (1989). Plant cell wall architecture. *Cell* **56**, 231–239.
- Weiser, R.L., Wallner, S.J., and Waddell, J.W.** (1990). Cell wall and extensin mRNA changes during cold acclimation of pea seedlings. *Plant Physiol.* **93**, 1021–1026.
- Wyss, U., Grundler, F.M.W., and Münch, A.** (1992). The parasitic behaviour of second-stage juveniles of *Meloidogyne incognita* in roots of *Arabidopsis thaliana*. *Nematologica* **38**, 98–111.
- Ye, Z.-H., and Varner, J.E.** (1991). Tissue-specific expression of cell wall proteins in developing soybean tissues. *Plant Cell* **3**, 23–37.